

Effect of Antiferroquadrupolar Interaction on the Magnetic Structure of $\text{Ho}^{11}\text{B}_2\text{C}_2$

Aya TOBO, Hiroki YAMAUCHI, Hideya ONODERA, Kenji OHOYAMA and Yasuo YAMAGUCHI

Institute for Materials Research, Tohoku University, Sendai, 980-8577, Japan

Tetragonal HoB_2C_2 shows an antiferroquadrupolar order transition at $T_Q = 4.5$ K, which is below the antiferromagnetic transition temperature $T_N = 5.9$ K. Between T_Q and T_N , there exists an intermediate phase, phase IV, which is a pure magnetic ordered phase. We have done the neutron diffraction measurements on a single crystal sample of $\text{Ho}^{11}\text{B}_2\text{C}_2$ in phase IV under zero magnetic field. In phase IV the system has a magnetic structure with a long periodicity, which is described by the two propagation vectors $\mathbf{k}_1 = [1\ 0\ 0]$ and $\mathbf{k} = [1+\delta\ \delta\ \delta']$. This configuration is expressed as a combination of equal magnetic moment component and longitudinal sinusoidal moment modulation.

KEYWORDS: HoB_2C_2 , antiferroquadrupolar ordering, antiferromagnet, magnetic structure, neutron diffraction

§1. Introduction

The systems showing both of an antiferroquadrupolar (AFQ) ordering and an antiferromagnetic (AFM) ordering have been attracting many interests. They are known to show complicated magnetic behavior because of competition and coexistence of AFQ order and AFM order. Among those systems, the most extensively studied ones are the cubic compounds CeB_6 and $\text{Ce}_x\text{La}_{1-x}\text{B}_6$, especially since a new phase, named phase IV, was discovered in $\text{Ce}_x\text{La}_{1-x}\text{B}_6$.^{1,2)} However, the nature of phase IV is still mysterious, because Kondo screening competes with quadrupolar and magnetic interactions in these systems.³⁾

Recently, it has been reported that DyB_2C_2 shows both an AFQ order transition and an AFM order transition.⁴⁾ DyB_2C_2 crystallizes in the tetragonal LaB_2C_2 -type structure (the space group $P4/mbm$).^{5,6)} The structure can be described as that the Dy layers and the B-C layers are piled up alternately along the c -axis. The most striking feature of DyB_2C_2 is the value of transition temperatures, besides being the first example of tetragonal compound showing an AFQ ordering. The AFQ order transition in DyB_2C_2 occurs at $T_Q = 24.7$ K, and the AFM order transition at $T_N = 15.3$ K. They are almost ten times as high as those of the other AFQ systems reported so far.

HoB_2C_2 , which has the same crystalline structure as DyB_2C_2 , also shows both of an AFQ ordering and an AFM ordering.⁷⁾ In HoB_2C_2 , the AFQ order transition occurs at $T_Q = 4.5$ K.⁸⁾ Amazingly, this transition occurs below the AFM transition temperature $T_N = 5.9$ K. Unlike $\text{Ce}_x\text{La}_{1-x}\text{B}_6$ mentioned above, phase IV of HoB_2C_2 is an AFM ordered phase without doubt.

From powder neutron diffraction pattern, Ohoyama *et al.* deduced the magnetic structure of $\text{Ho}^{11}\text{B}_2\text{C}_2$ at low temperature in zero magnetic field.¹⁰⁾ Here B was replaced with enriched ^{11}B isotope for the neutron diffraction measurements, because natural B is a strong neutron absorber. The magnetic structure below 4.5 K in

the coexistent phase of the AFQ order and the AFM order (phase III) is described by four propagation vectors of $\mathbf{k}_1 = [1\ 0\ 0]$, $\mathbf{k}_2 = [0\ 1\ 1/2]$, $\mathbf{k}_3 = [0\ 0\ 0]$ and $\mathbf{k}_4 = [0\ 0\ 1/2]$. The magnetic moments of $6.4\ \mu_B$ lie in the c -planes. Adjacent magnetic moments along the $[0\ 0\ 1]$ direction are placed at an angle of 70° with each other. In the c -plane, each magnetic moment makes an angle of about 150° with the nearest magnetic moment. Basically, the magnetic structure is explained by the overlap of AFQ $[0\ 0\ 1/2]$ structure and AFM $[1\ 0\ 0]$ structure. This ground state of HoB_2C_2 is essentially the same as that of DyB_2C_2 in the coexistent phase of AFQ order and AFM order, except the value of the angles between adjacent magnetic moments.

On the other hand, for $T_Q < T < T_N$ the AFM order is clearly observed with the powder neutron diffraction measurements. The magnetic structure is described by two propagation vectors: one of them is $\mathbf{k}_1 = [1\ 0\ 0]$, and the other is \mathbf{k} that indicated phase IV is a magnetic ordered state with long periodicity.¹⁰⁾ Possible propagation vector \mathbf{k} for a long periodicity is $\mathbf{k} = [1+\delta\ \delta\ 0]$ type or $\mathbf{k} = [1+\delta\ \delta\ \delta']$ type. The powder neutron diffraction measurements suggest $\mathbf{k} = [1+\delta\ \delta\ \delta']$, where $\delta \sim 0.11$ and $\delta' \sim 0.04$. However, determination of the precise magnetic structure remains ambiguous because of broadness and weakness of magnetic reflections. To confirm the suggestion from powder neutron diffraction measurements, we show the results of neutron diffraction measurements on the single crystal $\text{Ho}^{11}\text{B}_2\text{C}_2$ in phase IV.

§2. Experimental

The polycrystal $\text{Ho}^{11}\text{B}_2\text{C}_2$ were synthesized by the conventional argon arc technique. The mixture of appropriate proportions of 99.9 % pure Ho, 99.5 % enriched ^{11}B and 99.999 % pure C was melted, and the ingot was turned over and remelted several times. A single crystal was grown by the Czochralski method using a tri-arc furnace. We cut the single crystal with the size of about 6 mm \times 4 mm \times 1 mm. The mass of the sample is 47.1 mg. Neutron diffraction experiments were performed using

the KINKEN Single Crystal Diffractometer (KSD) installed at JRR-3M at the Japan Atomic Energy Research Institute. Neutron beam with wavelength of 1.527 Å was obtained by the 311 reflection of the Ge monochromator of vertical bent and 12'-∞-40' collimation. The single crystal sample was sealed in a standard aluminum cell with helium gas. The sample cell was mounted at the cold head of a closed-cycle He-gas refrigerator.

§3. Experimental Results

Firstly, we examined the neutron scattering intensity around magnetic Bragg peaks in the reciprocal a^*-a^* plane of the single crystal $\text{Ho}^{11}\text{B}_2\text{C}_2$ at 4.9 K, where $T_Q < 4.9 \text{ K} < T_N$. In Fig. 1(a), we show the contour plot of magnetic scattering intensity around reciprocal lattice position (1 0 0) in the reciprocal a^*-a^* plane. In the figure, we make a solid line every 5 contour lines. In order to make the height of intensity clear, we show two sets of profiles of h -scan along $(h 0 0)$ and $(h -0.1 0)$ in Fig. 1(b). The clear peak is observed at (1 0 0) magnetic Bragg point. Near (1 0 0) Bragg point, four small peaks are observed at $(1+\delta \delta 0)$, $(1+\delta -\delta 0)$, $(1-\delta +\delta 0)$ and $(1-\delta -\delta 0)$, where $\delta \sim 0.11$. These four small peaks have almost the same peak intensity. The peaks indicate that the magnetic structure in phase IV has long periodicity whose propagation vector \mathbf{k} is described by $[1+\delta \delta 0]$ type or $[1+\delta \delta']$ type.

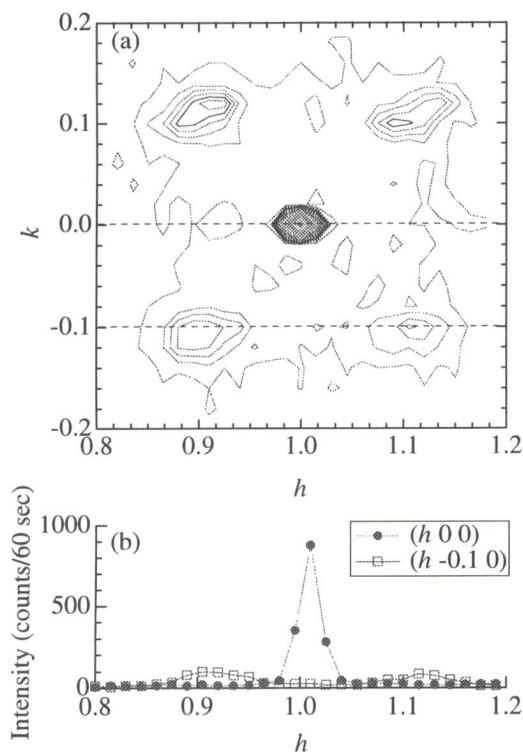


Fig. 1. Magnetic scattering intensity around the reciprocal lattice point (1 0 0) at 4.9 K of the single crystal HoB_2C_2 . (a) The contour plot of the magnetic scattering intensity in the reciprocal a^*-a^* plane. (b) Profiles of h -scan along $(h 0 0)$ and $(h -0.1 0)$.

To investigate the direction of the long periodicity component, we examined the neutron scattering intensity at the reciprocal lattice position (2 1 0). We show the contour plot of magnetic scattering intensity around reciprocal lattice position (2 1 0) in the reciprocal a^*-a^* plane in Fig. 2(a). We can see five peaks in the figure: a peak at (2 1 0) Bragg point, and four peaks surrounding it, like those around (1 0 0) Bragg point. However, the intensity of the peaks at $(2\pm\delta 1\mp\delta 0)$ is clearly larger than that of the peaks at $(2\pm\delta 1\pm\delta 0)$. In Fig. 2(b), we show two sets of profiles of h -scan along $(h 1 0)$ and $(h 0.9 0)$ to compare the intensity of the peaks. In consideration of the relation between propagation vector \mathbf{k} and scattering vector \mathbf{Q} at each reciprocal lattice point, this difference in intensity of the satellite peaks indicates that the direction of the magnetic moments of this long periodicity component is along $[1 1 0]$.

Next we show the correlation around magnetic Bragg peaks in the a^*-c^* plane of the single crystal HoB_2C_2 . In order to catch the satellite peaks, the vertical a -axis was tilted by 5.1°. In Fig. 3, profiles of l -scan along $(0.985 0.09 l)$ and $(0.91 0.08 l)$ at 5.2 K of the single crystal HoB_2C_2 . For the l -scan along $(0.985 0.09 l)$, a peak at reciprocal lattice position (1 0 0) is observed as seen in Fig. 3(a). On the other hand, for the l -scan along $(0.91 0.08 l)$, two broad peaks are observed as seen in Fig. 3(b). If the propagation vector \mathbf{k} describing the

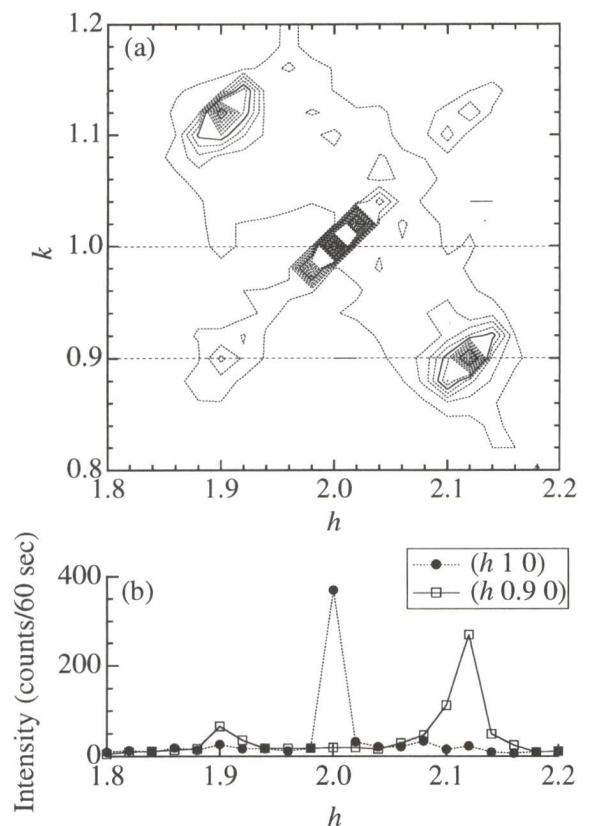


Fig. 2. Magnetic scattering intensity around the reciprocal lattice point (2 1 0) at 4.9 K of the single crystal HoB_2C_2 . (a) The contour plot of the magnetic scattering intensity in the reciprocal a^*-a^* plane. (b) Profiles of h -scan along $(h 1 0)$ and $(h 0.9 0)$.

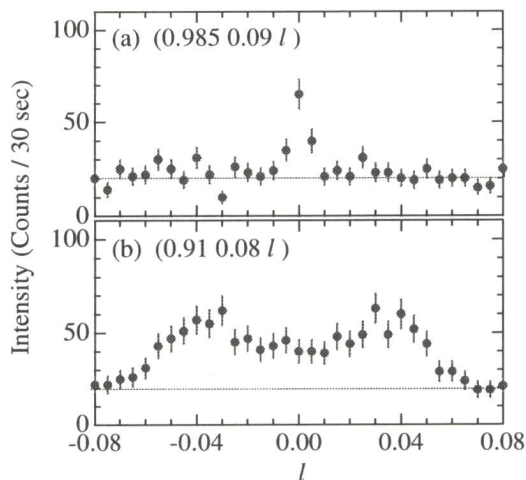


Fig. 3. Neutron magnetic scattering profiles of the single crystal HoB₂C₂ at 5.2 K. (a) l -scan along $(0.985\ 0.09\ l)$, and (b) l -scan along $(0.91\ 0.08\ l)$. In order to catch the satellite peaks, the a -axis was tilted by 5.1° .

long periodicity is $[1+\delta\ \delta\ 0]$ type, the profile for the l -scan along $(0.91\ 0.08\ l)$ shows only one peak around $l = 0$. The profiles with two peaks indicate that the propagation vector \mathbf{k} is surely $[1+\delta\ \delta\ \delta']$ type. From the peak positions, we obtained $\delta' \sim 0.04$.

§4. Discussion and Summary

From these measurements, we summarize the magnetic structure of HoB₂C₂ in phase IV as follows. In order to describe the antiferromagnetic structure of phase IV, two propagation vectors $\mathbf{k}_1 = [1\ 0\ 0]$ and $\mathbf{k} = [1+\delta\ \delta\ \delta']$ are needed. Here $\delta \sim 0.11$ and $\delta' \sim 0.04$. The propagation vector \mathbf{k}_1 corresponds to a simple antiferromagnetic coupling in the c -plane. The other propagation vector \mathbf{k} corresponds to a long periodicity with the magnetic moment of this component being $[1\ 1\ 0]$ direction. Because the magnetic moments are perpendicular to the c -axis, this long periodical \mathbf{k} means longitudinal sinusoidal moment modulation.

In Fig. 4, we show the most probable magnetic structure model of HoB₂C₂ in phase IV in the c -plane. We plotted the two arrows describing the magnetic moment of the each Ho atom. Actual magnetic moments are combination of the two components. One of them indicates the equal magnetic moment component, and the other indicates longitudinal sinusoidal moment modulation. In the adjacent c -plane, there exist the same equal moment configuration and longitudinal sinusoidal moment modulation that periodical modulation is shifted for the one twenty-fifth considered from the value of δ' . This magnetic structure is consistent with the results deduced by neutron powder diffraction measurements in ref. 10, in which the magnetic moment is roughly estimated to be $3\ \mu_B$.

Although no AFQ long-range order is observed in phase IV of HoB₂C₂, it is highly probable that the AFQ

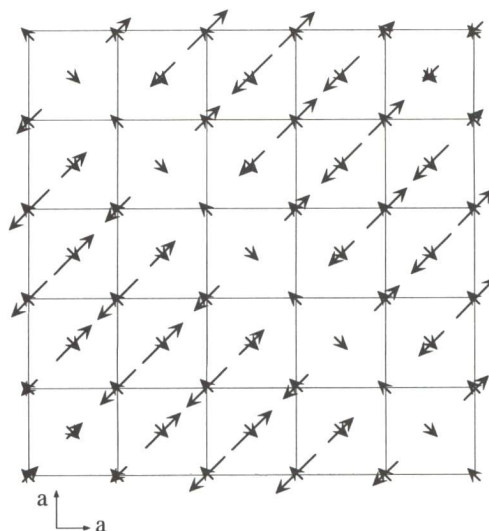


Fig. 4. Magnetic structure model of HoB₂C₂ in phase IV in the c -plane. Actual magnetic moment is the combination of the two components that is expressed as two arrows on each Ho atom. One of them indicates equal magnetic moment component, and the other indicates longitudinal sinusoidal moment modulation.

interactions affect the configuration of magnet moments. These AFQ interactions may cause the long periodicity of the magnetic structure in phase IV. To obtain further knowledge of the effect of AFQ interactions and its mechanism, we are planning detailed elastic neutron scattering and inelastic scattering measurements.

Acknowledgements

We would like to thank Mr. K. Nemoto of IMR, Tohoku University for the helpful assistance in the neutron scattering measurements. This work was partly supported by a Grant-in-Aid for Scientific Research (No. 12304017) from the Japan Society for the Promotion of Science.

- 1) H. Hiroi, M. Sera, N. Kobayashi and S. Kunii: Phys. Rev. B **55** (1997) 8339.
- 2) T. Tayama, T. Sakakibara, K. Tenya, H. Amitsuka and S. Kunii: J. Phys. Soc. Jpn. **66** (1997) 2268.
- 3) O. Suzuki, T. Goto, S. Nakamura, T. Matsumura and S. Kunii: J. Phys. Soc. Jpn. **67** (1998) 4243.
- 4) H. Yamauchi, H. Onodera, K. Ohoyama, T. Onimaru, M. Kosaka, M. Ohashi and Y. Yamaguchi: J. Phys. Soc. Jpn. **68** (1999) 2057.
- 5) T. Onimaru, H. Onodera, K. Ohoyama, H. Yamauchi and Y. Yamaguchi: J. Phys. Soc. Jpn. **68** (1999) 2287.
- 6) K. Kaneko, K. Ohoyama, H. Onodera and Y. Yamaguchi: submitted to J. Phys. Soc. Jpn.
- 7) H. Onodera, H. Yamauchi and Y. Yamaguchi: J. Phys. Soc. Jpn. **68** (1999) 2526.
- 8) Although in ref. 7 it was reported that $T_N = 5.8\ \text{K}$ and $T_Q = 5.0\ \text{K}$, we use newly obtained values of transition temperatures that are redefined by heat capacity data.⁹⁾
- 9) H. Shimada, H. Onodera, H. Yamauchi, A. Tobo, K. Ohoyama and Y. Yamaguchi: submitted to J. Phys. Soc. Jpn.
- 10) K. Ohoyama, H. Yamauchi, A. Tobo, H. Onodera, H. Kawawaki and Y. Yamaguchi: J. Phys. Soc. Jpn. **69** (2000) 3401.